European Journal of Medicinal Chemistry 62 (2013) 754–763

Contents lists available at SciVerse ScienceDirect

European Journal of Medicinal Chemistry

journal homepage: http://www.elsevier.com/locate/ejmech

Original article

Structure-based drug design using GPCR homology modeling: Toward the discovery of novel selective CysLT2 antagonists

Xiaowu Dong [a], Yanmei Zhao [a], Xueqin Huang [b], Kana Lin [b], Jianzhong Chen [a], Erqing Wei [b], Tao Liu [a,*], Yongzhou Hu [a,*]

[a] ZJU-ENS Joint Laboratory of Medicinal Chemistry, College of Pharmaceutical Sciences, Zhejiang University, Hangzhou 310058, China
[b] Department of Pharmacology, School of Medicine, Zhejiang University, Hangzhou 310058, China

ARTICLE INFO

Article history:
Received 15 November 2012
Received in revised form
16 January 2013
Accepted 24 January 2013
Available online 9 February 2013

Keywords:
G-protein-coupled receptors
CysLT2 antagonists
Homology model
Molecular docking
Structure-based design

ABSTRACT

3D structure of CysLT2 receptor was constructed by using homology modeling and molecular simulations. The binding pocket of CysLT2 receptor and the proposition of the interaction mode between CysLT2 and HAMI3379 were identified. A series of dicarboxylated chalcones was then virtually evaluated through molecular docking studies. A total of six compounds **13a**–**f** with preferable scores was further synthesized and tested for CysLT2 antagonistic activities by determination of the cytosolic free Ca^{2+} levels in HEK293 cells. Compounds **13e** and **13f** exhibited potent and selective CysLT2 antagonistic activities with IC_{50} values being 7.5 and 0.25 μM, respectively.

1. Introduction

Cysteinyl leukotrienes (CysLTs) LTC4, LTD4, and LTE4 are inflammatory mediators derived from arachidonic acid. They are generated in response to different immune and inflammatory stimuli [1–4], and exert biological effects via two major classes of receptors: CysLT1 and CysLT2 [5]. The physiological roles of CysLT1 receptor, which are coherent with anti-bronchoconstrictive and anti-inflammatory activities of CysLT1 antagonists, such as pranlukast [6], montelukast [7] and zafirlukast [8], are well documented [9] (Fig. 1A). In contrast, the pharmacological role of CysLT2 receptor is yet less defined due to the lacking of specific antagonists. Several previously identified nonselective CysLT1/CysLT2 receptor antagonists, such as BAY u9773 [10] and DUO-LT [11], were commonly used as tools to characterize the physiological roles of CysTL2 receptor, while the poor selectivity and weak potency of these antagonists hampered further progresses. HAMI3379 (Fig. 1B) was recently reported as the potent and selective CysLT2 receptor antagonist that can effectively reverse the LTC4-induced perfusion pressure increase and contractility decrease in isolated Langendorff-perfused guinea pig hearts [12]. Thus, CysLT2 receptor may relate to cerebral spinal fluid (CSF) circulation in leukotrienes-dependent vascular reactions, thus, being a potential target for treatment of cardiovascular disease. However, there have been no reports delineating the structure–activities relationships of HAMI3379 derivatives and possible interaction modes between CysLT2 and HAMI3379.

Although the X-ray crystal structure of CysLT2 has not been revealed yet, the bovine rhodopsin (bRh)-based homology modeling has been a well-established approach to study 3D structures of the GPCR receptors [13,14]. Previously, site-directed mutagenesis has been applied to the elucidation the structures of P2Y receptors [15,16], which showed close structural and phylogenetic relationships between P2Ys and CysLTs [17]. Recently, Parravicini et al. reported the molecular modeling of GPR17 receptor, a G-protein-coupled receptor located at intermediate phylogenetic position between two distinct receptor families: the P2Ys and CysLTs receptors [18,19]. These methods and results provided useful guidance in the construction of 3D structure of CysLT2 receptor.

A series of monocarboxylated chalcones (e.g. compounds **7** and **8**, Fig. 2A) was previously identified as good CysLT1 antagonists [20], and none of them exhibited CysLT2 antagonistic activities (Supplementary Table S1). This study was consistent with reported result that CysLT2 receptor was not sensitive to classical CysLT1 antagonists [21,22]. A review of the structures of reported CysLT2

* Corresponding authors. Tel./fax: +86 571 88208460.
E-mail addresses: lt601@zju.edu.cn (T. Liu), huyz@zju.edu.cn (Y. Hu).

0223-5234/$ – see front matter © 2013 Elsevier Masson SAS. All rights reserved.
http://dx.doi.org/10.1016/j.ejmech.2013.01.041

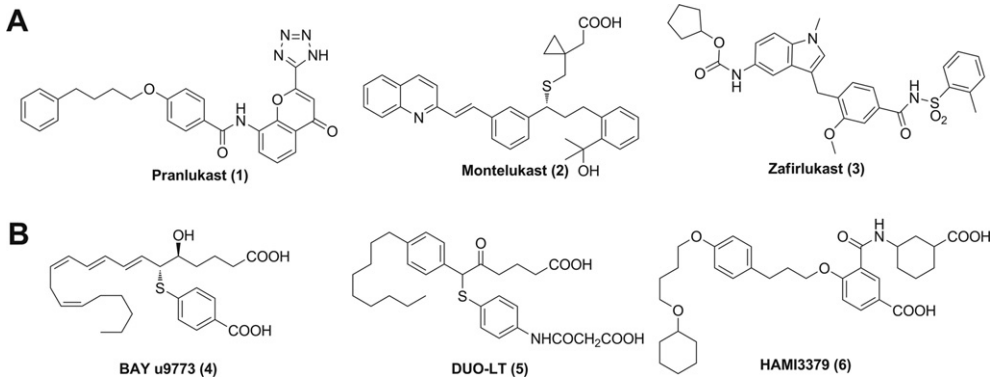

Fig. 1. Structures of CysLT1 antagonists (A) and CysLT2 antagonists (B).

antagonists revealed several common features among CysLT2 antagonists that are concluded and highlighted as shown in Fig. 2B. Thus, two carboxyl groups were introduced onto the A-ring of chalcones and a lipophilic chain was introduced on the B-ring of chalcones to give dicarboxylated chalcones as potential CysLT2 antagonists (Fig. 2C). Herein, with the aim to enhance accuracy and efficiency in the development of novel CysLT2 antagonists, 3D structure of CysLT2 was constructed through homology modeling and dynamic simulations. The binding pocket of CysLT2 was defined and the interaction mode between CysLT2 and HAMI3379 was proposed. The newly designed dicarboxylated chalcones were then virtually evaluated by molecular docking and preferable screened hits **13a**–**f** were synthesized and biologically evaluated for CysLT2 antagonistic activities.

2. Computational methods

2.1. Homology modeling

The amino acidic sequences of CysLT2, *b*Rh and pharmacological related CysLT1 and P2Y1,4,6 receptors were obtained from Swiss-Prot/TrEMBL database (http://expasy.org/). At first, we aligned the CysLT2 sequence with the other GPCRs' sequences using automatic alignment tool in Discovery studio 2.5 (Accelrys, Inc. San Diego, CA). Manual multiple sequence alignments (Fig. 3) were then conducted to locate the homology aligned regions taking into account both primary and secondary structures according to reported literature [18,23], in which the authors constructed a reliable homology model for GPR17, a G-protein-coupled receptor located at the intermediate phylogenetic position between two distinct receptor families: P2Ys and CysLTs receptors. Moreover, two conserved disulphide bridges (Cys111–Cys187 and Cys31–Cys279) were proposed, since that these disulfide bonds were considered as an important factor in constraining the conformation of the extracellular and transmembrane domains of the receptor. Finally, homology modules of the Discovery Studio 2.5 program were applied to build an initial approximate 3D structure of CysLT2 receptor, while the first high resolution structure of bovine rhodopsin (PDB ID: 1U19) [24] was used as a template.

2.2. Hydrophobic profile analysis

Since the hydrophobic residues for GPCRs tend to be buried in the interior of the protein and the hydrophilic residues are more exposed to cellular membrane, a profile of these values can indicate the overall folding pattern. Herein, we applied Kyte–Doolittle (KD)

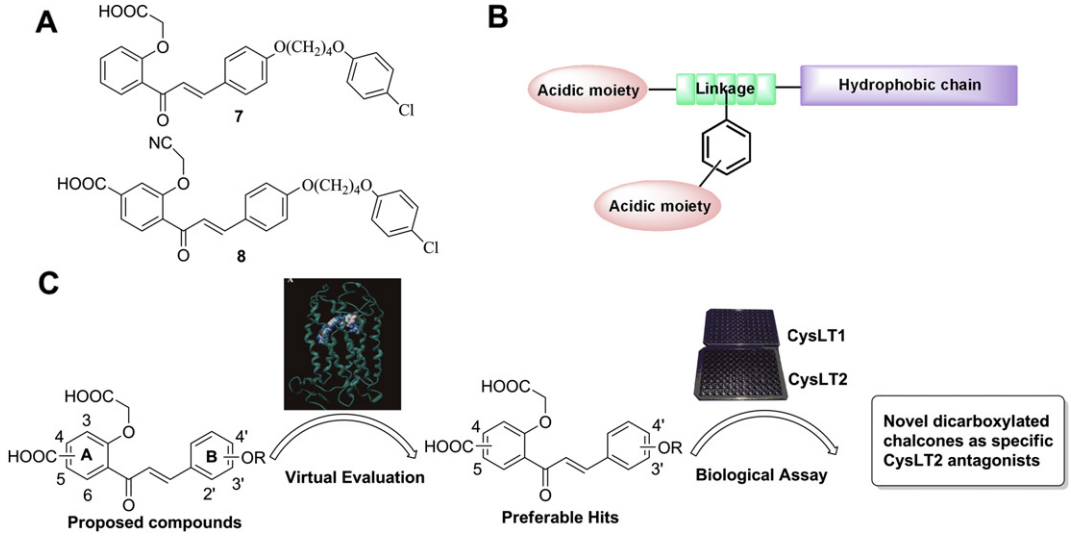

Fig. 2. Rational design and development of dicarboxylated chalcone derivatives as CysLT2 antagonists, A) the structure of identified monocarboxylated chalcones **7** and **8** as CysLT1 antagonists in our previous study [20]; B) the common structural features of CysLT2 antagonists; C) the evolution of dicarboxylated chalcone derivatives as novel specific CysLT2 antagonists.

Fig. 3. Multiple alignment of the sequences of bovine rhodopsin (bRh), CysLT2, CysLT1 and P2Y1,4,6 receptors. The cysteines involved in the formation of the two assumed disulphide bridges are highlighted in blue; the conserved residues and motif are highlighted in green.(For interpretation of the references to colour in this figure legend, the reader is referred to the web version of this article.)

method [25], a widely used technique for detecting hydrophobic regions in proteins, to perform the hydrophobic profile analysis of the identified transmembrane regions by visualizing the hydrophobicity of CysLT2 along its sequence. As defined in the Kyte–Doolittle scale, the hydrophobicity is calculated by sliding a fixed size window (size = 9) over the protein sequence. At the central position of the window, the average hydrophobicity of the entire windows is plotted.

2.3. Protein/membrane complex building process

The crude model of CysLT2 receptor was locally minimized using CHARMM force field [26] *in vacuo* by constraining the backbone of the helices in order to give a first optimization of the rough geometry derived from homology modeling. The model of DPPC in the liquid-crystalline phase proposed by Tieleman and Berendsen [27,28] was used to produce the membrane environment. The structure of CysLT2 was inserted in the centre of the 128 lipid bilayer using membrane Builder in the CHARMM-GUI website [29], in such a way that the principal axes of the helical bundle was parallel to the membrane axis (z) and perpendicular to the membrane plane (xy), and the extracellular and intracellular loops were at the lipid interface. The resulting complex system consisted of 346 amino acid residues, 122 DPPC molecules, 10,305 water molecules, for a total of 52,279 atoms in a rectangular box of $62 \times 78 \times 92$ Å.

2.4. Molecular dynamics simulations

The final ensemble was submitted to energy minimization cycles, followed by simulated annealing in order to lead the system to a more favorable energetic condition before starting the pure MD simulation, the backbone of the seven TM helices and the structured EL-2 motifs were constrained to maintain the overall arrangement of the helical bundle and the structural conserved organization of EL-2. The protocol by which the assembly was prepared for the MD run was composed of separated cycles as described below. For the earlier minimization steps, the steepest descent algorithm was applied. The minimization sequence of the various component of the system was the following: first the lipids, then the water, then both lipids and water, and finally the whole system. Then, further the conjugate gradient algorithm was used to minimize the whole system, and then a first run of 200 ps of MD simulation at 5 K was performed. At the end of this first minimization and relaxation protocol, a simulated annealing procedure was performed as follows. The system was heated from 5 to 310 K in 400 ps, and kept at this temperature for further 240 ps. Then, an MD simulation with CHARMM force field was performed at

a temperature of 310 K for a total of 3 ns of dynamics simulation without any constraints.

2.5. Molecular docking and MM/MD simulation

2.5.1. Molecular docking with LigandFit [30] program

The docking site of CysLT2 receptor was derived using the LigandFit site search utility in Discovery studio 2.5 [30]. For the generation of the ligand's conformations, we used variable numbers of Monte Carlo simulations. All the calculations during the docking steps were performed under the PLP Force Field formalism. A short rigid body minimization was then performed and 50 poses for each ligand were saved. Scoring was performed with a set of scoring functions (including Dock_score, -PLP1 and -PMF) implemented in LigandFit module. The combination of consensus scoring method and the interaction mode was applied to select the preferable output conformation.

2.5.2. Molecular docking with Flexidock [31] program

The binding pocket was defined all residues within 4 Å of the ligand within the CysLT2 complex proposed by LigandFit. All single bonds of residue side chains inside the binding pocket were regarded as rotatable or flexible. The docked ligand was allowed to rotate on all of single bonds and move flexibly within the tentative binding pocket. The obtained enzyme–ligand complex was further minimized with 500 iterations of steepest descent and followed by a conjugate gradients optimization by using CHARMM force field within Discovery Studio 2.5 program. Then, the binding energy [32] between CysLT2 receptor and its bound ligand was calculated using "Calculate binding energies module" in Discovery studio 2.5 program

$$E_{\text{int}} = E(A,B) - (E(A) + E(B)),$$

where $E(A)$ and $E(B)$ are the energies of CysLT2 and ligand respectively, and $E(A,B)$ the energy of docked complex.

2.5.3. MD/MM simulation on HAMI3379-bound CysLT2 complex

The HAMI3379-bound CysLT2 complex proposed by Flexidock study was further refined by molecular dynamic and mechanical (MD/MM) calculations, with aim to examine the reliability of the interaction mode of HAMI3379: (a) An NVT ensemble molecular dynamic simulations with CHARMM force field were then performed at a constant temperature of 300 K with a time step of 1 fs for a total of 1.5 ns, while atomic constraints of backbone of CysLT2 were applied to retain; (b) the output conformation was initially run with CHARMM force field for 500 iterations of steepest descents, followed by a 500 iterations conjugate gradients optimization. The other parameters of MD/MM simulation are maintained at their Discovery studio default configuration.

3. Results and discussion

3.1. The initial crude structure of CysLT2 receptor

3.1.1. Seven TM helices bundle

As shown in Fig. 4, the results from Kyte–Doolittle (KD) analysis indicated that the hydrophobic properties of the amino acid residues of CysLT2 were consistent with the structural features of seven transmembrane domains. The amino acid residues from seven TM helices (from TM1 to TM7) are much more hydrophobic, since that these residues tend exposed to cellular membrane and result in formation of a complex weave of polar interactions. It has been demonstrated that there are close structural and phylogenetic relationships between the P2Ys and CysLTs families which have been characterized by consisting of the seven TM helices bundle (TM1-7), an extracellular *N*-terminus region (NT), a cytoplasmic *C*-terminus tail (CT) and three extracellular (ECs) and three intracellular (ICs) loops [33,34].

3.1.2. Conserved residues and motifs

The amino acid sequences of both CysLT1 and CysLT2 receptors have only 24–32% identity to members of the purinergic (P2Y) receptor family, however, several conserved structural motifs of these nucleotide receptors (e.g. CysLTs and P2Ys receptors) were readily found, especially in the nucleotides bound domains (EC1, TM2, TM3 and TM6) [23,35]. The conserved domains of these receptors are highlighted in Fig. 3, including a WXFG motif in the first extracellular loop (EC1) of each receptor, a hydrophobic motif (VXMXNLAXXDLL) in the second transmembrane domain (TM2), a YVNXY motif in the third transmembrane domain (TM3) and a conserved HXXRT motif in the sixth transmembrane domain (TM6). Therefore, all of them were taken into consideration in manual multi-sequence alignment, homology modeling and molecular simulation.

3.1.3. Disulfide bond bridge

The disulfide bonds play important role in constraining the conformation of extracellular domains of the protein and stabilize the transmembrane structures [36,37]. As commonly found in others' GPCR receptors, the outmost part of TM3 of CysLT2 seemed to be permanently engaged in a conserved disulphide bridge with

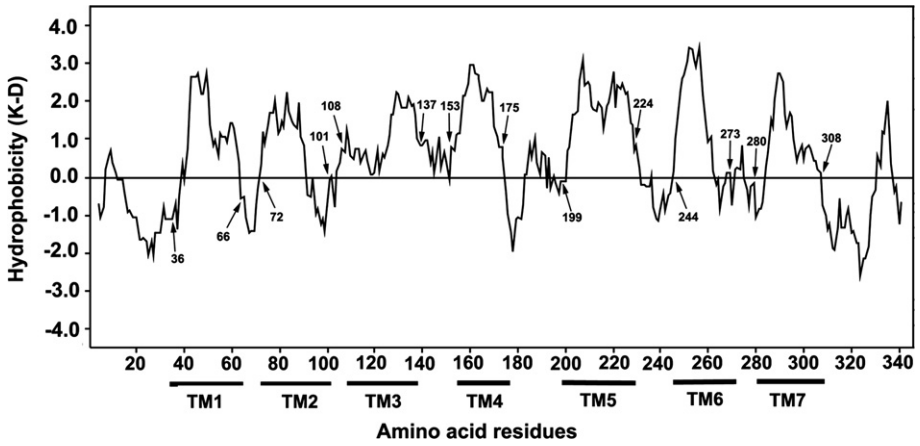

Fig. 4. Plot of hydrophobicity along the amino acid sequence for CysLT2 receptor by using Kyte–Doolittle analysis, window size = 9, max = 3.50, min = −2.75.

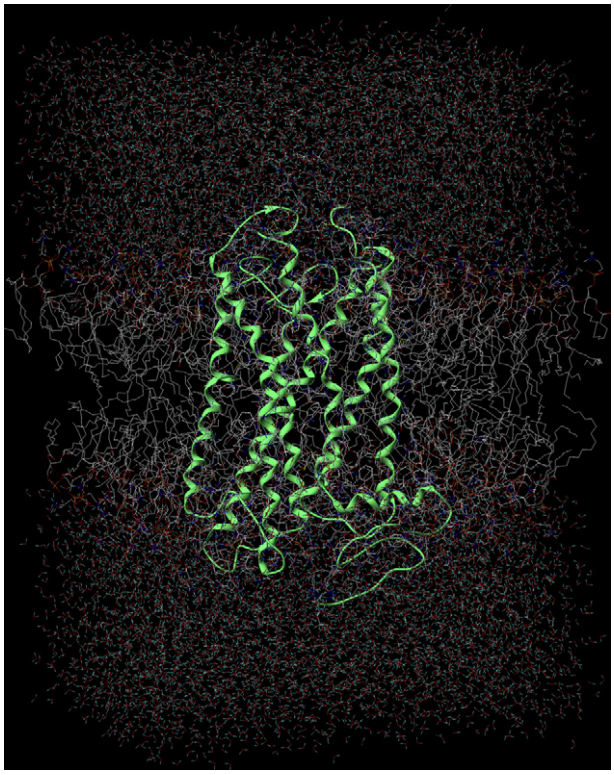

Fig. 5. Typical structure of CysLT2 embedded in the fully hydrated lipid bilayer. A frame of the system extracted from the 3 ns MD simulations is shown. The helix and loops of CysLT2 are represented in green, the DPPC are in orange and white, water is in red/blue.(For interpretation of the references to colour in this figure legend, the reader is referred to the web version of this article.)

EC2 of CysLT2 involving the Cys111 and Cys187 residues. In addition, CysLT2 has another pair of cysteines which are conserved in all the P2Ys and CysLTs receptors; these two residues are positioned at the end of the Nt (Cys31) and at the middle of the EC3 domain (Cys279), respectively. It has been demonstrated by site-directed mutagenesis and ligand affinity data that corresponding cysteines in P2Y1 form a disulphide bridge which is important for receptor activation [38]. Thus, we also included this additional disulphide bridge into the 3D structure of CysLT2 receptor.

3.2. Homology model refined by molecular simulation

3.2.1. Molecular dynamics within protein/membrane complex

The locally minimized structure was embedded in a fully hydrated phospholipidic bilayer (dipalmitoylphosphatidylcholine, DPPC, hydrated with water). The structure of the protein–lipids–solvent system derived from the simulated annealing simulation was used as input for 3 ns of molecular dynamics. After an initial decrease, the total energy of the system kept a stable trend, indicating that an equilibrium state had been reached (Supplementary Fig. S1). The final picture of the protein after 3 ns of MD is shown in Fig. 5. It reveals that the 346 amino acids of CysLT2 fold into seven transmembrane helices, three extracellular and three intracellular loops, as well as a cytoplasmic helix. The inter-helix hydrogen bond and non-bonded interactions were observed that are essential for the stabilization of the seven transmembrane domains of CysLT2 receptor structure. For example, TM3 positions itself in close contact with the TM2, TM4, TM5 and TM7 through inter-helix hydrogen bonds (e.g., Ser117–Leu91, Asn121–Asp84, Tyr95–Gly181, Tyr99–Val180, Asn93–Asn269). Other hydrogen bond interactions were also detected including TM1 with adjacent TM7 (Try17–Leu263, Asn28–Ala270), TM2 with adjacent TM3, TM4 and TM7 (Ser117–Leu91, Asn121–Asp84, Leu52–Trp135, Asp56–Asn273). Besides, the hydrogen bonds between EL-2 and TM1, TM3 and TM6 (e.g. Ser155–Arg10, Cys159–Met86, Glu161–Tyr91, Leu162–Arg267, Asn163– His242) play important role in stabilization of the seven transmembrane domains. Also, non-bonded inter-helix interactions, such as the hydrophobic interaction between non-polar side chains of each pair of adjacent helices, including $\pi-\pi$ interaction (e.g. Phe41–Tyr45, Phe87–Tyr116–Tyr163, Phe93–Tyr97–Phe106, Phe214–Phe257 and Tyr301–Phe312–Tyr302) and lots of hydrophobic alkyl–alkyl interaction (e.g. Leu129–Leu117–Leu253, Val131–Leu158–Ile162, Leu132–Ile249, Val53–Leu85–Ile60, Leu206–Leu271–Thr268, Leu224–Ile250–Leu244 and Ile251–Ile255–Leu304).

3.2.2. Definition of the binding site

On the basis of the homology-constructed CysLT2 structure, LigandFit/active site finding module was applied to find the most promising binding domains, which is located in a cavity among the TM1, TM3, and TM5–TM7 on the extracellular side of the seven TMs bundles. This cavity consists of a hydrophilic center pointed toward

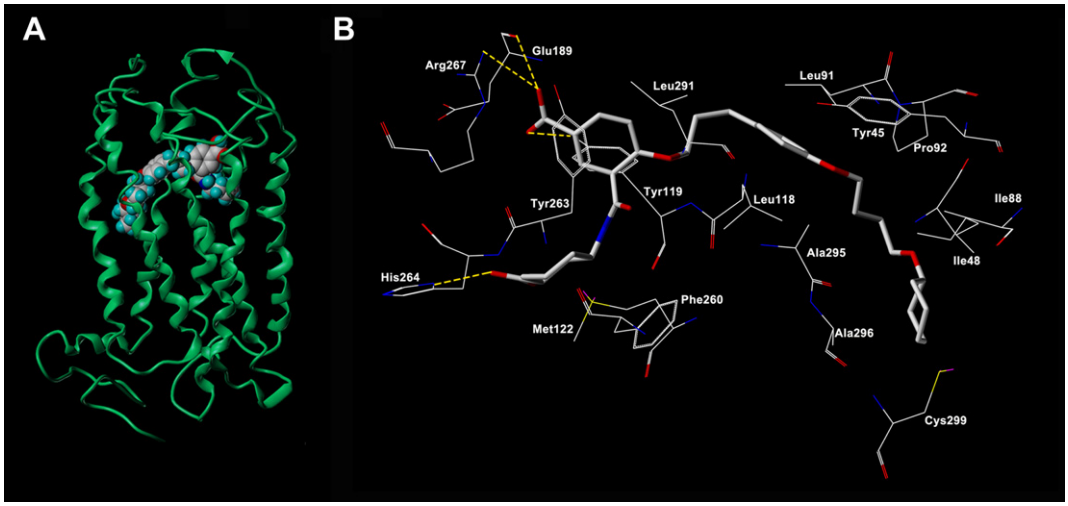

Fig. 6. Model of the complex formed by CysLT2 receptor and HAMI3379 after 1 ns of MD simulation. (A) HAMI3379 is displayed as spheres in the schematic representation of the entire ligand–receptor complex; (B) HAMI3379 is displayed in stick within the binding pocket of CysLT2 in the detailed picture, and the polar interactions between HAMI3379 and CysLT2 are highlighted using yellow dash line.(For interpretation of the references to colour in this figure legend, the reader is referred to the web version of this article.)

the TM6 and EL-2 domains (His264, Arg267 and Glu189) and a large hydrophobic cleft surrounded by hydrophobic residues (Leu118, Ala295, Ala296, Ala298, Cys299 and Ile48). The distance between the hydrophilic and hydrophobic centers of the identified cavity is estimated to be 15–17 Å, which is approximately typical size of a CysLT2 antagonist, such as the HAMI3379. Furthermore, the defined binding pocket is also congruent with the biochemical studies, by comparing with observed characteristics of other transmembrane receptors (*e.g.* bovine Rhodopsin [37] and P2Y1 [38]). As found in P2Y1, both His277 and Lys280 are essential for ligand recognition and/or receptor activation [15,39]. In our constructed CysLT2 structure, these two crucial residues are His264 and Arg267, which would be critical to the binding affinity of CysLT2 ligands. The interaction analysis between TM6 and adjacent helices also validated the binding cavity of CysLT2, since that TM6 engaged only few interactions with other helices. It is suggested that this helix may maintain a dynamic behavior needed to evoke receptor activation without constraints from the other helices. In fact, in *b*Rh, TM6 is believed to move away from TM3 thereby starting the activation process [40].

3.2.3. The interaction mode between CysLT2 and HAMI3379

The overall picture of the CysLT2 and HAMI3379 complex (Fig. 6A) was obtained by means of molecular dynamics (MD) runs of 1 ns starting from the best-docked conformation of CysLT2 and HAMI3379 proposed by LigandFit and followed by Flexidock. A total energy of the system kept a stable trend, indicating that an equilibrium state had been reached (Supplementary Fig. S2). The putative arrangement of HAMI3379 in CysLT2 binding site is displayed in Fig. 6B. The guanidine group of Arg267 seems to form an ionic bond with carboxyl on the phenyl group of HAMI3379 (C=O–Arg267: 2.89Å), while the imidazol group of His264 seems to form another ionic bond interaction with carboxyl group on cyclohexane moiety of HAMI3379 (C–O–His264: 2.97Å). A hydrogen bond between the carboxyl group on the phenyl group of HAMI3379 with the hydroxyl group of Tyr119 (C=O–Tyr119: 2.02Å) was observed to form another hydrophilic interaction. In addition to the polar interactions, hydrophobic contacts were also found within the pocket: these involved hydrophobic resides Leu291, Leu93, Leu118, Ala295, Ala296, Ala298 and Cys299, and aromatic residues Try119, Tyr263 and Tyr45. Although holding some peculiar features, the overall configuration of the bound ligand agreed with the general configuration reported in previous computational study for P2Y receptors [41]. Furthermore, these interactions (such as polar and non-polar interactions) were further analyzed in the time evolution of HAMI3379-bound CysLT2 complex using molecular dynamic simulation (Supplementary Fig. S3A–C), showing all of the interactions are stable and would be essential for ligand binding.

3.3. Evaluation of dicarboxylated chalcones through molecular docking

Once the HAMI3379-bound CysLT2 complex was obtained, the newly designed dicarboxylated chalcones were virtually evaluated using molecular docking by combination of LigandFit and Flexidock. At first, the LigandFit was used to fast examine the fitness between the shape of the dicarboxylated chalcones and topological feature of the binding pocket of CysLT2. Then, the Flexidock, an advanced molecular docking program, was applied to investigate more accurate binding mode between CysLT2 and screened hits. It is indicated that 4(or 5)-carboxyl group on A-ring and more than eight atomic alkyl chain on B-ring of chalcones are preferable for their interacting with CysLT2. Then, a total of six promising hits **13a**–**f** (Fig. 7) was picked out considering the good docking scores,

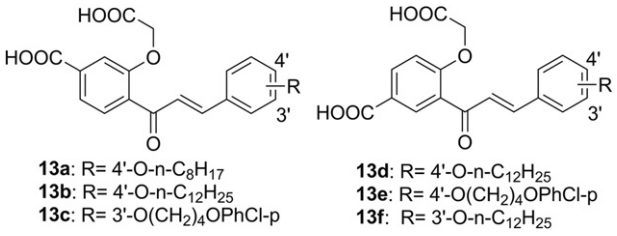

Fig. 7. Structures of promising hits **13a**–**f** identified by docking studies.

structural diversity and synthetic feasibility. The docking results of them are shown in Table 1. All of them show good consensus results, with good performance in more than three scoring functions. As exemplified by **13f**, the best one predicted in docking studies, the dock scores, -PLP1 and -PMF (Dock_score: 136.6; -PLP1: 145.9 and -PMF: 191.9) obtained from LigandFit are promising and comparable to that of HAMI3379 (Dock_score: 153.0; -PLP1: 164.9 and -PMF: 209.0). Also, the result of Flexidock indicated that the compound **13f** showed the lowest interaction energy (−411.7 kcal/mol), which is even lower than that of HAMI3379 (−377.0 kcal/mol). Furthermore, the synthesis and biological evaluation of screened hits **13a**–**f** with good docking results were performed to validate robustness and predictive ability of the homology model as well as molecular docking.

3.4. Chemistry

The synthetic route for compound **13** is outlined in Scheme 1. Claisen–Schmidt condensation of acetophenone **9** with appropriate benzaldehyde **10** in the presence of 10% potassium hydroxide in a solvent of EtOH-THF-H_2O (5:5:2) for 5–6 days, following by the esterization with ethanol in the presence of sulfuric acid afforded chalcone **11**. Alkylation of **11** with ethyl bromoacetate in the presence of potassium carbonate and acetone gave in **12**, which was further alkaloid hydrolyzed using 5% sodium hydroxide in EtOH–H_2O mixture solvent at room temperature to get dicarboxylated chalcone **13**.

3.5. Pharmacological activities

The CysLT2 antagonistic potency of the screened hits **13a**–**f** was evaluated by determination of cytosolic free Ca^{2+} levels in HEK293 cells which were stably transfected with pcDNA3.1 (+)-hCysLT2. In this biological evaluation model, PT-PCR and Western blot analysis showed a higher expression of $CysLT_2$ receptor in HEK293 cells (Supplementary Fig. S4). ATP at 50 μM significantly elevated $[Ca^{2+}]_i$, and was used as a positive control for measurement of $[Ca^{2+}]_i$. LTD_4 at 0.1 μM also significantly increased $[Ca^{2+}]_i$, which could be partially blocked by Bay u9773 (a CysLT1 and CysLT2 dual antagonist) but could not blocked by selective CysLT1 receptor antagonists

Table 1
The docking results of screened hits **13a**–**f** and reference **HAMI3379**.

Compd.	LigandFit			Binding energy (kcal/mol)
	Dock_score	-PLP1	-PMF	
HAMI3379	153.0	164.9	209.0	−377.0
13a	119.9	125.4	188.0	−312.7
13b	122.8	131.2	175.4	−378.8
13c	120.8	133.4	166.2	−390.4
13d	128.9	134.9	184.1	−262.6
13e	127.2	130.1	205.9	−298.8
13f	136.6	145.9	191.9	−411.7

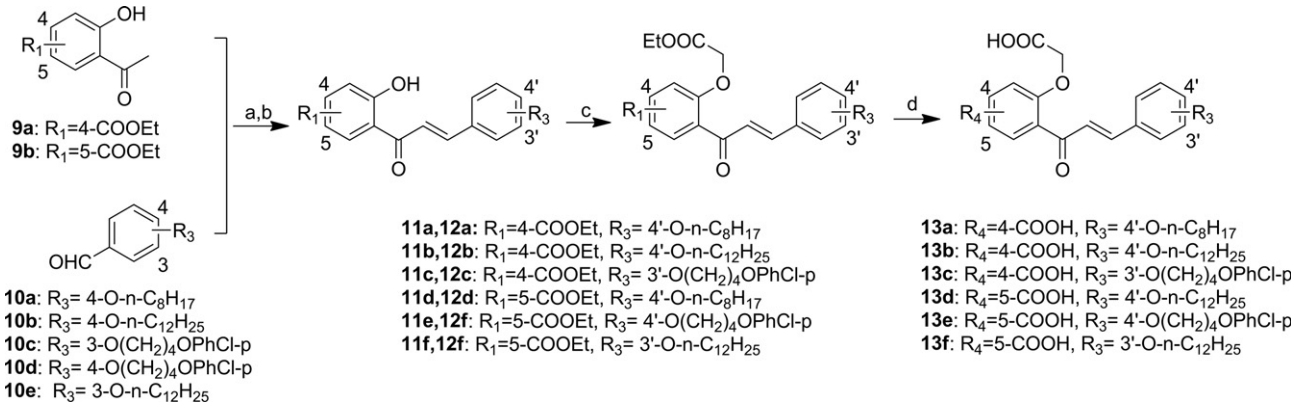

Scheme 1. Synthesis of dicarboxylated chalcones **13a**–**f**. Reagents and conditions:(a) appropriate alkyl bromide, K_2CO_3, acetone; (b) 10% KOH, ethanol/THF/H_2O, r.t.; (c) H_2SO_4, EtOH; (d) $BrCH_2COOEt$, K_2CO_3, acetone, reflux; (e) 5% NaOH, EtOH/H_2O.

montelukast and pranlukast (CysLT1 antagonists). As shown in Fig. 8A, the antagonistic effects of tested compounds **13a**–**f** at a concentration of 1 μM were observed, especially for compounds **13e** and **13f**, which show 44.0% and 70.5% decreased $[Ca^{2+}]_i$ by blocking the agonistic effect of LTD4, respectively. As shown in Fig. 8B, the antagonistic effects of **13e** and **13f** were observed in a dose-dependent manner with the maximal effect (**13e** and **13f**: 72.8% and 80.5%, respectively), and their half antagonistic concentration are also good ($IC_{50}$of **13e** and **13f**: 7.5 and 0.25 μM, respectively). In order to examine the selective profiles of the tested compounds **13a**–**f** against CysLT1 and CysLT2 receptors, the CysLT1 antagonistic activities of them were evaluated according to our previous method [20]. The results demonstrated that the most promising compounds **13e** and **13f** also show good selectivity for CysLT2 receptor, while they exhibit very low antagonistic potency on CysLT1 receptor (Supplement Table S2). Thus, as expected, the introduction of two carboxyl groups onto the A-ring of chalcones is preferable for CysLT2 antagonistic activities, by comparing with our previous monocarboxylated chalcones (e.g. compounds **7** and **8**). By optimization of the length and substituents of the lipophilic chain on B-ring of chalcones can significantly modulate the CysLT2 antagonistic activities. Obviously, the homology model based structural modification of CysLT2 antagonists is a rational protocol, and can remarkably improve efficiency in lead optimization. Although monomonocarboxylated chalcones haven been reported as CysLT1 antagonists [20,42], it is also interestingly that the dicarboxylated chalcones are the firstly reported as CysLT2 antagonists.

3.6. Docking mode analysis of compound *13f*

The interaction mode of compound **13f** proposed by molecular docking studies is given in Fig. 9A and B. The binding pocket was rendered from the molecular surface color-coded by hydrophobicity (brown to blue: a scale of hydrophobic to hydrophilic properties). Overall, the interaction mode of **13f** is consistent with that of HAMI3379.A hydrophilic region (His264, Arg267 and Glu189) and a large hydrophobic cleft (Leu118, Ala295, Ala296, Ala298, Cys299 and Ile48) of the binding pocket of CysLT2 tightly embrace compound **13f** and form polar and non-polar interactions. The guanidine group of Arg267 and the imidazol group of His264 seem to form ionic bonds with two carboxyl group of **13f** (C=O–Arg267: 2.39Å, C=O–His264: 3.09Å). A further hydrogen bond is possibly established between the carboxyl oxygen atom of **13f** and the hydroxyl oxygen atom of Tyr119 (C=O–Tyr119: 2.23Å). Moreover, the presence of a significant hydrophobic cleft (Leu291, Leu93, Leu118,

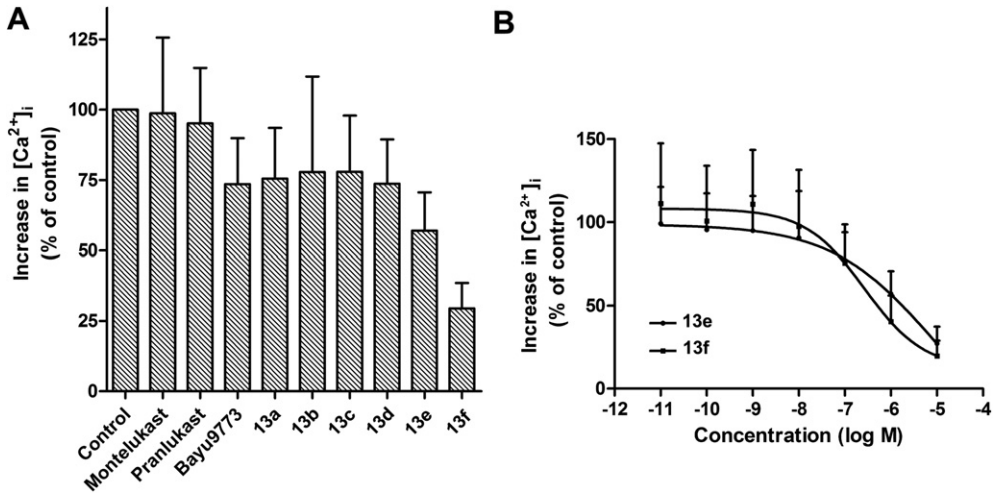

Fig. 8. The CysLT2 antagonistic activities of tested compounds on the LTD4 (0.1 μM)-elevated $[Ca^{2+}]^i$ in HEK293 cells which were stably transfected with pcDNA3.1 (+)-hCysLT2. A) The CysLT2 antagonistic activities of dicarboxylated chalcones **13a**–**f**, montelukast, pranlukast and bay u9773 at a concentration of 1 μ; B) the concentration–dependent CysLT2 antagonistic activities of **13e** and **13f**.

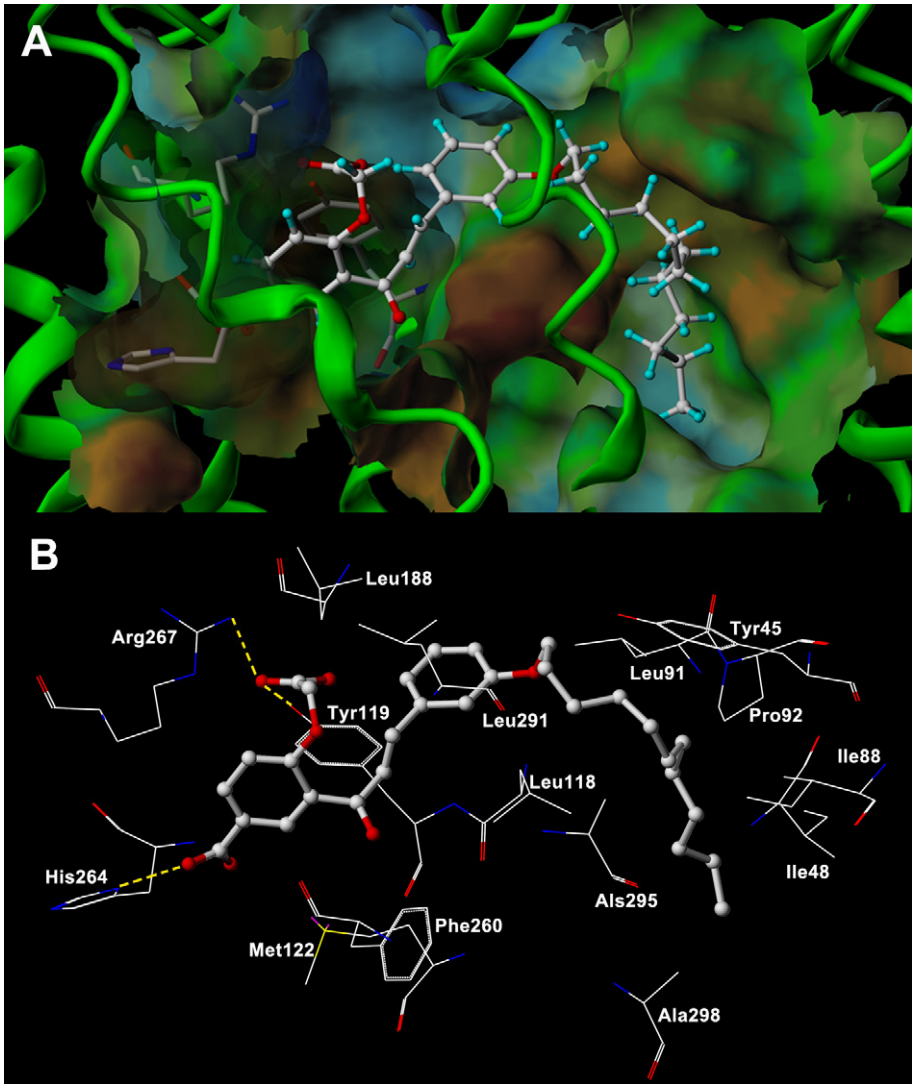

Fig. 9. Interaction mode of **13f** (CysLT2 antagonistic $IC_{50} = 0.25$ μM) with CysLT2 proposed by molecular docking. A) Compound **13f** was embraced in the CysLT2 binding pocket, which was rendered from the molecular surface and color-coded by hydrophobicity (brown to blue: a scale of hydrophobic to hydrophilic properties); B) **13f** is displayed in stick within the binding pocket of CysLT2 in the detailed picture, and the polar interactions between **l3f** and CysLT2 are highlighted using yellow dash line.(For interpretation of the references to colour in this figure legend, the reader is referred to the web version of this article.)

Ala295, Ala296, Ala298 and Cys299, Try45) in the CysLT2 binding site that is capable of accommodating a long hydrophobic chain on B-ring of chalcone. In addition, the aromatic stack interaction between the phenol ring of Tyr119 and A-ring of **13f** also serves to increase the thermal stability of the complex.

4. Conclusion

The 3D structure of CysLT2 was established using homology modelling and applied in virtually evaluation of newly designed dicarboxylated chalcones using molecular docking. This approach led to the identification of six promising screened hits **13a**–**f**, which were synthesized and biologically evaluated for CysLT2 antagonistic activities. The identification of compounds **13e** and **13f** with good and selective CysLT2 antagonistic activities indicated that combination of homology model and structure-based development of novel specific CysLT2 antagonists is a rational strategy. The interaction mode between CysLT2 and its ligands proposed in present study would be useful and valuable for further structural optimization of CysLT2 antagonists. To the best of our knowledge, the homology model of CysLT2 receptor and its application in structure-based lead optimization are reported for the first time. Also, the discovery of novel dicarboxylated chalcones, such as compounds **13e** and **13f**, as CysLT2 antagonists would be interesting leads to do further structure–activity exploration and structurally optimization.

5. Experimental

5.1. Chemistry

For experimental procedures and spectral characterization data see the Supplementary Material.

5.2. CysLT2 antagonistic activities

The CysLT2 antagonistic potency of the test compounds was evaluated by determination of cytosolic free Ca^{2+} levels in HEK293 cells which were stably transfected with pcDNA3.1 (+)-hCysLT2 [43]. In brief, cells were seeded in 96-well culture plates (BMG

LABTECHNOLOGIES 96) and grown at 37 °C in 5% CO_2-containing humidified air. Twenty-four hours after plating, the growth medium was removed and replaced with 50 μl BSS (BSS in mM: NaCl 140, KCl 4, $MgCl_2$ 1, $CaCl_2$ 1.25, HEPES 5, glucose 11, NaH_2PO_4 1, ascorbic acid 5.7; pH 7.4) containing 1 μM Fluo4 AM and 0.03% pluronic F-127 for 45 min at 37 °C. After loading, Fluo4 AM was removed and cells were washed three times with BSS. Then 40 μl BSS containing tested compounds or not were added to the wells and cells were further incubated for 30 min. After that, cells were transferred to the FLUOstar OPTIMA (BMG Germany) and 50 μM ATP which as a positive stimulus or 0.1 μM LTD4 was added to the wells. Calcium concentration ($[Ca2^+]_i$) was measured as the fluorescence monitored at 37 °C (485 nm excitation, 525 nm emission) and the LTD4 response was obtained by calculating peak minus basal fluorescence values, and reported as percentages of control values (BSS only).

Acknowledgements

The authors are grateful to the support provided by the National Natural Science Foundation of China (No. 81001359) and the China Postdoctoral Science Foundation (No. 201003734) and the Fundamental Research Funds for the Central Universities (No. 2011QNA7010).

Appendix A. Supplementary data

Supplementary data related to this article can be found at http://dx.doi.org/10.1016/j.ejmech.2013.01.041.

References

[1] S. Poulin, C. Thompson, M. Thivierge, S. Veronneau, S. McMahon, C.M. Dubois, J. Stankova, M. Rola-Pleszczynski, Cysteinyl-leukotrienes induce vascular endothelial growth factor production in human monocytes and bronchial smooth muscle cells, Clin. Exp. Allergy 41 (2011) 204–217.
[2] E. Mayatepek, G.F. Hoffmann, Leukotrienes: biosynthesis, metabolism, and pathophysiologic significance, Pediatr. Res. 37 (1995) 1–9.
[3] K.F. Chung, Leukotriene receptor antagonists and biosynthesis inhibitors: potential breakthrough in asthma therapy, Eur. Respir. J. 8 (1995) 1203–1213.
[4] H.E. Claesson, S.E. Dahlen, Asthma and leukotrienes: antileukotrienes as novel anti-asthmatic drugs, J. Intern. Med. 245 (1999) 205–227.
[5] R.A. Coleman, R.M. Eglen, R.L. Jones, S. Narumiya, T. Shimizu, W.L. Smith, S.E. Dahlen, J.M. Drazen, P.J. Gardiner, W.T. Jackson, et al., Prostanoid and leukotriene receptors: a progress report from the IUPHAR working parties on classification and nomenclature, Adv. Prostaglandin Thromboxane Leukot. Res. 23 (1995) 283–285.
[6] S.H. Yoo, S.H. Park, J.S. Song, K.H. Kang, C.S. Park, J.H. Yoo, B.W. Choi, M.H. Hahn, Clinical effects of pranlukast, an oral leukotriene receptor antagonist, in mild-to-moderate asthma: a 4 week randomized multicentre controlled trial, Respirology 6 (2001) 15–21.
[7] G.L. Yu, E.Q. Wei, M.L. Wang, W.P. Zhang, S.H. Zhang, J.Q. Weng, L.S. Chu, S.H. Fang, Y. Zhou, Z. Chen, Q. Zhang, L.H. Zhang, Pranlukast, a cysteinyl leukotriene receptor-1 antagonist, protects against chronic ischemic brain injury and inhibits the glial scar formation in mice, Brain Res. 1053 (2005) 116–125.
[8] S.L. Spector, Management of asthma with zafirlukast. Clinical experience and tolerability profile, Drugs 52 (Suppl. 6) (1996) 36–46.
[9] V. Capra, Molecular and functional aspects of human cysteinyl leukotriene receptors, Pharmacol. Res. 50 (2004) 1–11.
[10] M. Back, Functional characteristics of cysteinyl-leukotriene receptor subtypes, Life Sci. 71 (2002) 611–622.
[11] H. Galczenski, J. Hutchinson, D.J. Figueroa, J. Scheigetz, R. Young, J.F. Evans, American Thoracic Society, in: 98th International Conference (May 2002, Atlanta) [D38] [Poster F4] Characterization of DUO-LT: A Novel Dual Cysteinyl Receptor Antagonist.
[12] F. Wunder, H. Tinel, R. Kast, A. Geerts, E.M. Becker, P. Kolkhof, J. Hutter, J. Erguden, M. Harter, Pharmacological characterization of the first potent and selective antagonist at the cysteinyl leukotriene 2 (CysLT(2)) receptor, Br. J. Pharmacol. 160 (2010) 399–409.
[13] S. Moro, F. Deflorian, G. Spalluto, G. Pastorin, B. Cacciari, S.K. Kim, K.A. Jacobson, Demystifying the three dimensional structure of G protein-coupled receptors (GPCRs) with the aid of molecular modeling, Chem. Commun. (Camb) (2003) 2949–2956.
[14] A.M. Van Rhee, B. Fischer, P.J. Van Galen, K.A. Jacobson, Modelling the P2Y purinoceptor using rhodopsin as template, Drug Des. Discov. 13 (1995) 133–154.
[15] Q. Jiang, D. Guo, B.X. Lee, A.M. Van Rhee, Y.C. Kim, R.A. Nicholas, J.B. Schachter, T.K. Harden, K.A. Jacobson, A mutational analysis of residues essential for ligand recognition at the human P2Y1 receptor, Mol. Pharmacol. 52 (1997) 499–507.
[16] L. Erb, R. Garrad, Y. Wang, T. Quinn, J.T. Turner, G.A. Weisman, Site-directed mutagenesis of P2U purinoceptors. Positively charged amino acids in transmembrane helices 6 and 7 affect agonist potency and specificity, J. Biol. Chem. 270 (1995) 4185–4188.
[17] R. Fredriksson, M.C. Lagerstrom, L.G. Lundin, H.B. Schioth, The G-protein-coupled receptors in the human genome form five main families. Phylogenetic analysis, paralogon groups, and fingerprints, Mol. Pharmacol. 63 (2003) 1256–1272.
[18] C. Parravicini, G. Ranghino, M.P. Abbracchio, P. Fantucci, GPR17: molecular modeling and dynamics studies of the 3-D structure and purinergic ligand binding features in comparison with P2Y receptors, BMC Bioinform. 9 (2008) 263.
[19] I. Eberini, S. Daniele, C. Parravicini, C. Sensi, M.L. Trincavelli, C. Martini, M.P. Abbracchio, In silico identification of new ligands for GPR17: a promising therapeutic target for neurodegenerative diseases, J. Comput. Aided Mol. Des. 25 (2011) 743–752.
[20] X. Dong, L. Wang, X. Huang, T. Liu, E. Wei, L. Du, B. Yang, Y. Hu, Pharmacophore identification, synthesis, and biological evaluation of carboxylated chalcone derivatives as CysLT1 antagonists, Bioorg. Med. Chem. 18 (2010) 5519–5527.
[21] C.E. Heise, B.F. O'Dowd, D.J. Figueroa, N. Sawyer, T. Nguyen, D.S. Im, R. Stocco, J.N. Bellefeuille, M. Abramovitz, R. Cheng, D.L. Williams Jr., Z. Zeng, Q. Liu, L. Ma, M.K. Clements, N. Coulombe, Y. Liu, C.P. Austin, S.R. George, G.P. O'Neill, K.M. Metters, K.R. Lynch, J.F. Evans, Characterization of the human cysteinyl leukotriene 2 receptor, J. Biol. Chem. 275 (2000) 30531–30536.
[22] J. Takasaki, M. Kamohara, M. Matsumoto, T. Saito, T. Sugimoto, T. Ohishi, H. Ishii, T. Ota, T. Nishikawa, Y. Kawai, Y. Masuho, T. Isogai, Y. Suzuki, S. Sugano, K. Furuichi, The molecular characterization and tissue distribution of the human cysteinyl leukotriene CysLT(2) receptor, Biochem. Biophys. Res. Commun. 274 (2000) 316–322.
[23] E.A. Mellor, A. Maekawa, K.F. Austen, J.A. Boyce, Cysteinyl leukotriene receptor 1 is also a pyrimidinergic receptor and is expressed by human mast cells, Proc. Natl. Acad. Sci. U.S.A. 98 (2001) 7964–7969.
[24] T. Okada, M. Sugihara, A.N. Bondar, M. Elstner, P. Entel, V. Buss, The retinal conformation and its environment in rhodopsin in light of a new 2.2 Å crystal structure, J. Mol. Biol. 342 (2004) 571–583.
[25] J. Kyte, R.F. Doolittle, A simple method for displaying the hydropathic character of a protein, J. Mol. Biol. 157 (1982) 105–132.
[26] B.R. Brooks, R.E. Bruccoleri, B.D. Olafson, D.J. States, S. Swaminathan, M. Karplus, CHARMM – a program for macromolecular energy, minimization, and dynamics calculations, J. Comput. Chem. 4 (1983) 187–217.
[27] D.P. Tieleman, H.J.C. Berendsen, molecular dynamics simulations of a fully hydrated dipalmitoylphosphatidylcholine bilayer with different macroscopic boundary conditions and parameters, J. Chem. Phys. 105 (1996) 4871–4880.
[28] D.P. Tieleman, S.J. Marrink, H.J. Berendsen, A computer perspective of membranes: molecular dynamics studies of lipid bilayer systems, Biochim. Biophys. Acta 1331 (1997) 235–270.
[29] S. Jo, T. Kim, W. Im, Automated builder and database of protein/membrane complexes for molecular dynamics simulations, PLoS One 2 (2007) e880.
[30] C.M. Venkatachalam, X. Jiang, T. Oldfield, M. Waldman, LigandFit: a novel method for the shape-directed rapid docking of ligands to protein active sites, J. Mol. Graph. Model. 21 (2003) 289–307.
[31] T. Ahnfeldt, D. Gunzelmann, T. Loiseau, D. Hirsemann, J. Senker, G. Ferey, N. Stock, Synthesis and modification of a functionalized 3D open-framework structure with MIL-53 topology, Inorg. Chem. 48 (2009) 3057–3064.
[32] R. Vijayalakshmi, V. Subramanian, B.U. Nair, A study of the interaction of Cr(III) complexes and their selective binding with B-DNA: a molecular modeling approach, J. Biomol. Struct. Dyn. 19 (2002) 1063–1071.
[33] F. Horn, J. Weare, M.W. Beukers, S. Horsch, A. Bairoch, W. Chen, O. Edvardsen, F. Campagne, G. Vriend, GPCRDB: an information system for G protein-coupled receptors, Nucleic Acids Res. 26 (1998) 275–279.
[34] F. Horn, E. Bettler, L. Oliveira, F. Campagne, F.E. Cohen, G. Vriend, GPCRDB information system for G protein-coupled receptors, Nucleic Acids Res. 31 (2003) 294–297.
[35] D.T. Major, B. Fischer, Molecular recognition in purinergic receptors. 1. A comprehensive computational study of the h-P2Y(1)-receptor, J. Med. Chem. 47 (2004) 4391–4404.
[36] S.S. Karnik, H.G. Khorana, Assembly of functional rhodopsin requires a disulfide bond between cysteine residues 110 and 187, J. Biol. Chem. 265 (1990) 17520–17524.
[37] K. Palczewski, T. Kumasaka, T. Hori, C.A. Behnke, H. Motoshima, B.A. Fox, I. Le Trong, D.C. Teller, T. Okada, R.E. Stenkamp, M. Yamamoto, M. Miyano, Crystal structure of rhodopsin: a G protein-coupled receptor, Science 289 (2000) 739–745.
[38] C. Gerard, C. Mollereau, G. Vassart, M. Parmentier, Nucleotide sequence of a human cannabinoid receptor cDNA, Nucleic Acids Res. 18 (1990) 7142.
[39] A.A. Ivanov, I. Fricks, T. Kendall Harden, K.A. Jacobson, Molecular dynamics simulation of the P2Y14 receptor. Ligand docking and identification of a putative binding site of the distal hexose moiety, Bioorg. Med. Chem. Lett. 17 (2007) 761–766.

[40] J. Saam, E. Tajkhorshid, S. Hayashi, K. Schulten, Molecular dynamics investigation of primary photoinduced events in the activation of rhodopsin, Biophys. J. 83 (2002) 3097–3112.
[41] S. Costanzi, B.V. Joshi, S. Maddileti, L. Mamedova, M.J. Gonzalez-Moa, V.E. Marquez, T.K. Harden, K.A. Jacobson, Human P2Y(6) receptor: molecular modeling leads to the rational design of a novel agonist based on a unique conformational preference, J. Med. Chem. 48 (2005) 8108–8111.
[42] M.E. Zwaagstra, H. Timmerman, M. Tamura, T. Tohma, Y. Wada, K. Onogi, M.Q. Zhang, Synthesis and structure-activity relationships of carboxylated chalcones: a novel series of CysLT1 (LTD4) receptor antagonists, J. Med. Chem. 40 (1997) 1075–1089.
[43] V. Capra, S. Ravasi, M.R. Accomazzo, M. Parenti, G.E. Rovati, CysLT1 signal transduction in differentiated U937 cells involves the activation of the small GTP-binding protein Ras, Biochem. Pharmacol. 67 (2004) 1569–1577.